Chapter 2

Design and Optimal Location of Power System Stabilizer in the Multi-Machine Power Network

2.1 Introduction

This chapter proposes a Damping Torque Index (DTI) to determine the optimal installation location of the Power System Stabilizer (PSS) in the multi-machine power network. The proposed index is based on the Classical Damping Torque Analysis (CDTA) method for power system Low-Frequency Electro-Mechanical Oscillation (LFO) analysis. The selection criteria of the PSS location is the maximum magnitude of DTI under normal operating conditions. The CDTA method is used to design PSS, and the phase compensation technique subsequently adjusts the associated parameters. Furthermore, to analyze the power system's critical oscillation mode, a Wide-Area Damping Controller (WADC) is designed for the synchronous generator where the optimal location of PSS is installed. The reduced-order model-based WADC includes time-varying delay in the wide-area signal. The WADC's input signals are taken from the Phasor Measurement Unit (PMU) and the location of the PMU are selected using geometric measures of observability, and WADC parameters designed based on the residue approach. The proposed approach is validated in two separate test systems, and modal analysis is carried out on MATLAB software. The simulated results have been validated on the Real-Time Digital Simulator (RTDS) RSCAD 5.012. Results obtained on RTDS show that the proposed approach

efficiently damps low-frequency electro-mechanical oscillations.

2.2 Power System Modelling

2.2.1 Synchronous generator

Synchronous generators are characterized by a reduced-order flux decay model [64]:

$$\frac{d\delta_i}{dt} = \omega_i - \omega_s \tag{2.1}$$

$$\frac{2H_i}{\omega_s}\frac{d\omega_i}{dt} = T_{Mi} - E_{qi}^{'} I_{qi} - \left(X_{qi} - X_{di}^{'}\right) I_{di} I_{qi} - D\left(\omega_i - \omega_s\right) \tag{2.2}$$

$$T_{doi}^{'}\frac{E_{qi}^{'}}{dt} = -E_{qi}^{'} - \left(X_{di} - X_{di}^{'}\right) I_{di} + E_{fdi} \tag{2.3}$$

$$T_{Ai}\frac{E_{fdi}}{dt} = -E_{fdi} + K_{Ai}\left(V_{refi} - V_i\right) \tag{2.4}$$

for $i = 1, ..., m$, where m represents the total number of Synchronous Generator (SG) present in the system. The notation follows the nomenclature guidelines. A fourth-order flux decay model expresses each SG, and every SG has a fast static exciter.

2.2.2 PSS model

The primary objective of a PSS is to add damping to the SG rotor by monitoring its excitation system with supplementary stabilizing signals like SG rotor speed, power, or terminal frequency. The PSS improves the LFO by adding an electrical torque component (damping torque) phased with the SG rotor speed. Fig. 2.1 depicts the linearized structure of PSS.

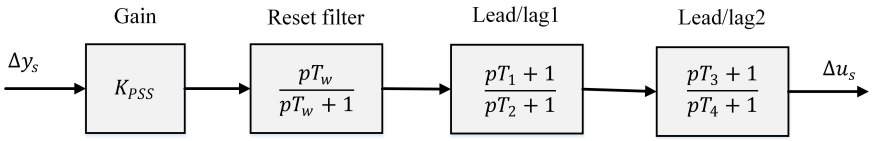

Figure 2.1: Structure of the PSS.

In Fig. 2.1 K_{PSS} represents the gain of the PSS, p imitate as a differential operant, the input signal is Δy_s and the output signal is Δu_s, which is emitted to the exciter,

T_1, T_2, T_3 and T_4 are lead-lag block time constant, and reset filter time constant isT_w. The phase adjustment is achieved with the lead/lag block, and the damping introduced by the PSS is determined by the gain. The PSS transfer function is obtained from Fig. 2.1 as,

$$T_{PSS(s)} = K_{PSS}\frac{pT_w}{pT_w+1}\frac{pT_1+1}{pT_2+1}\frac{pT_3+1}{pT_4+1} \tag{2.5}$$

2.3 Linearized Model for the Entire System

The linearized model of the Multi-Machine Power Network (MMPN) is used to analyze and control LFO in modern power systems. Considering incremental changes in variables and assuming PSS is connected to S^{th} SG, equation (2.1)-(2.4) is linearized about the steady-state operating point [65, 66].

$$\begin{bmatrix} \Delta\dot{\delta}_L \\ \Delta\dot{\omega}_L \\ \Delta\dot{E}_L \end{bmatrix} = \begin{bmatrix} 0 & \omega_0 I & 0 \\ K_L & D_L & A_{L23} \\ A_{L31} & A_{L32} & A_{L33} \end{bmatrix} \begin{bmatrix} \Delta\delta_L \\ \Delta\omega_L \\ \Delta E_L \end{bmatrix} + \begin{bmatrix} 0 \\ 0 \\ B_L \end{bmatrix} \Delta u_s \tag{2.6}$$

for $L = 1, 2, \ldots, m$, where δ_L is the SG load angle deviation, $\Delta\omega_L$ is the SG rotor speed deviation, ΔE_L represent state variables considering all the SG excluding the rotor speed and load angle variables, Δu_s is the deviation of damping signal from PSS, and B_L represents transfer function matrix from Δu_s to state variables.

The feedback signals y_S of the stabilizers can be obtained as

$$\Delta y_s = \begin{bmatrix} c_{1SL} & c_{2SL} & C_{3SL} \end{bmatrix} \begin{bmatrix} \Delta\delta_L \\ \Delta\omega_L \\ \Delta E_L \end{bmatrix} + d_{LS}\Delta u_s \tag{2.7}$$

The output of the PSS is represented as

$$\Delta U_s = T_{PSS}(s)\Delta Y_s \tag{2.8}$$

where ΔU_s and ΔY_s represent Laplace transform of Δu_s and Δy_s, respectively and $T_{PSS}(s)$ represents transfer function relating Δu_s and Δy_s. Equation (2.6)-(2.8) represents the state-space representation of an MMPN containing the PSS in the system. The block layout of the PSS-enabled linearized power system is illustrated in Fig. 2.2. In Fig. 2.2, s is the complex frequency, and I is a unity matrix.

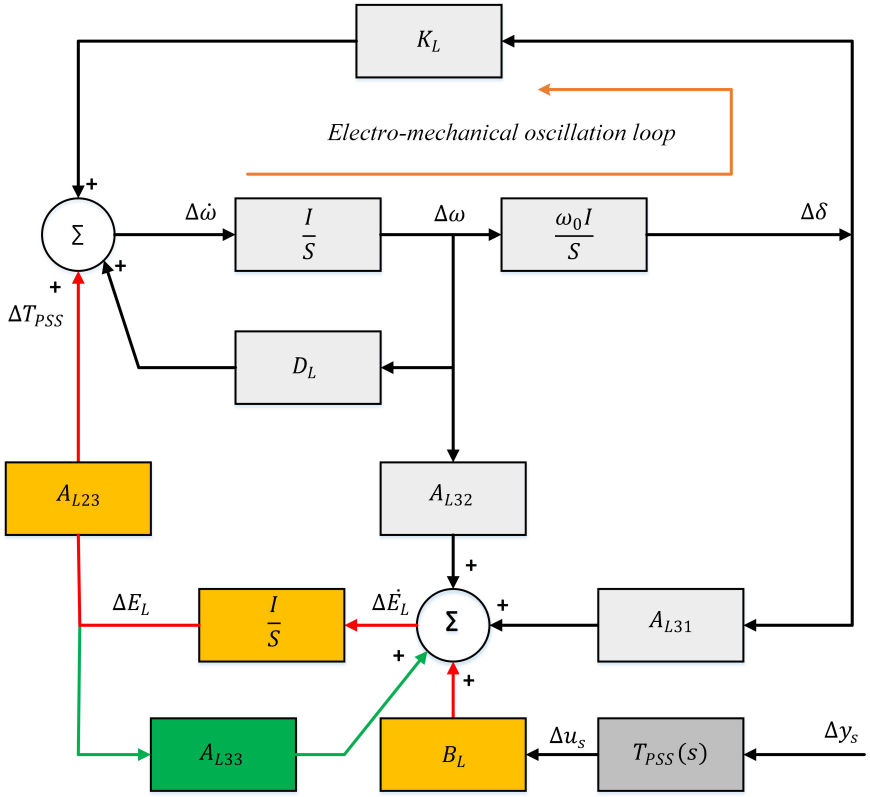

Figure 2.2: Block layout of PSS-enabled linearized power systems.

2.4 Classical Damping Torque Analysis Method

The preliminary study of the Classical Damping Torque Analysis (CDTA) method explains the detailed structure of Damping Torque added by the damping stabilizer in multi-machine power systems [65, 66, 67]. The forward path after the PSS controlling signal to the SG LFO loop is shown in Fig. 2.2 and can be characterized as follows:

$$F_{PSS}(s) = A_{L23}\left(sI - A_{L33}\right)B_L \tag{2.9}$$

The feedback signal ΔY_s can be reconstructed by SG rotor speed deviation as [65]

$$\Delta Y_s = \gamma_L(s)\omega_0\Delta\omega_L \tag{2.10}$$

where $\gamma_L(s)$ represent the reconstructed function. So

$$\Delta U_s = T_{PSS}(s)\gamma_L(s)\omega_0\Delta\omega_L \tag{2.11}$$

From (2.6), (2.8), and (2.10)

$$\Delta E_L = (sI - A_{L33})^{-1}\left[\frac{\omega_0}{s}A_{L31} + A_{L32} + B_L T_{PSS}(s)\gamma_L(s)\right]\omega_0\Delta\omega_L \tag{2.12}$$

From (2.8), (2.10), and (2.12)

$$\begin{aligned}\Delta Y_s = &\left(\frac{\omega_0}{s}c_{1sL} + c_{2sL}\right) + C_{3sL}\left(sI - A_{L33}\right)^{-1}\left(\frac{\omega_0}{s}A_{L31} + A_{L32}\right)\omega_0\Delta\omega_L \\ &\times \left[C_{3sL}\left(sI - A_{L33}\right)^{-1}B_L + d_{Ls}\right]T_{PSS}(s)\gamma_L(s)\omega_0\Delta\omega_L\end{aligned} \tag{2.13}$$

From (2.10), and (2.13)

$$\gamma_L(s) = \frac{\Delta y_s}{\omega_0\Delta\omega_L} \tag{2.14}$$

$$\gamma_L(s) = \frac{\left(\frac{\omega_0}{s}c_{1sL} + c_{2sL}\right) + C_{3sL}\left(sI - A_{L33}\right)^{-1}\left(\frac{\omega_0}{s}A_{L31} + A_{L32}\right)}{\left[C_{3sL}\left(sI - A_{L33}\right)^{-1}B_L + d_{Ls}\right]T_{PSS}(s)} \tag{2.15}$$

The damping torque produced by the PSS to the LFO loop of the L^{th} SG and k^{th} oscillation mode in the MMPN is determined from Fig. 2.2 and (2.9), and (2.11) as [65].

$$\Delta T_{PSSkL} = F_{PSS}(s)T_{PSS}(s)\Delta U_s \tag{2.16a}$$

$$= \left[F_{PSSL}\left(\lambda_k\right)\gamma_L\left(\lambda_k\right)T_{PSS}\left(\lambda_k\right)\right]\omega_0\Delta\omega_L \tag{2.16b}$$

$$= \left[T_L\angle\varphi_L T_{PSS}\left(\lambda_k\right)\right]\omega_0\Delta\omega_L \tag{2.16c}$$

$$= D_{PSSkL}\omega_0\Delta\omega_L \tag{2.16d}$$

where, λ_k is the critical LFO mode, $T_L\angle\varphi_L = F_{PSSL}\left(\lambda_k\right)\gamma_L\left(\lambda_k\right)$ and $D_{PSSkL} = [T_L\angle\varphi_L T_{PSS}\left(\lambda_k\right)]$.

The (2.16d) represents the PSS equipped in the power network to contribute to the damping torque, $D_{PSSkL}\omega_0\Delta\omega_L$ to LFO loop of each SG in the system. The sensitivity of λ_k to the addition of damping torque with the L^{th} SG can be defined as $S_{KL} = \frac{\partial\lambda_k}{\partial D_{PSSKL}}$ where the inclusion of damping torque, $D_{PSSkL}\omega_0\Delta\omega_L$ on each SG influences the LFO mode of interest. Therefore, the total enhancement of the LFO mode of interests λ_k by the power system damping stabilizer is defined as

$$\Delta\lambda_k = \sum_{J=1}^{m} D_{PSSkL}S_{kL} \tag{2.17}$$

Fig. 2.3 shows the result of (2.17). It depicts how the PSS adds damping torque to each SG and subsequently converts it to influence the essential LFO mode of interest. So, the Damping Torque Index(DTI) derived as

$$DTI_k = \frac{\Delta\lambda_k}{\Delta T_{PSS}\left(\lambda_k\right)} = \sum_{J=1}^{m}\left|S_{kL}T_L\angle\varphi_L\right| = \sum_{J=1}^{m}\left|F_{PSSL}\left(\lambda_k\right)\gamma_L\left(\lambda_k\right)T_{PSS}\left(\lambda_k\right)\right| \tag{2.18}$$

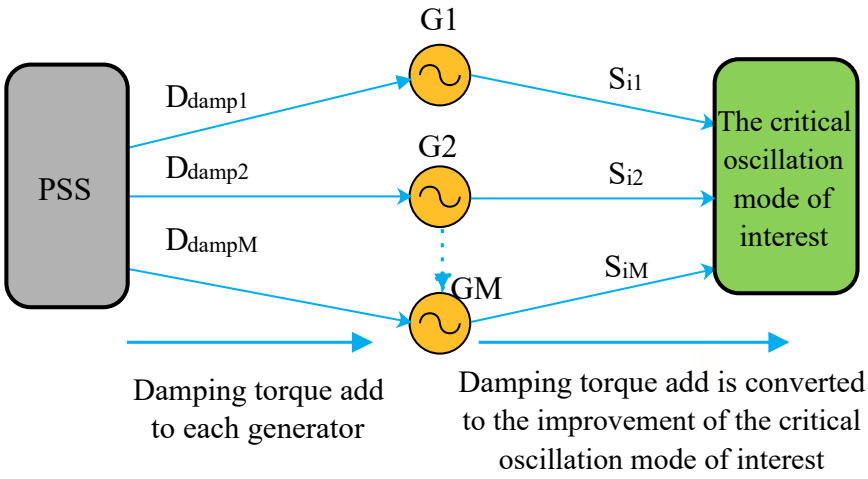

Figure 2.3: The critical oscillation mode of interest impressed by PSS.

The DTI explains the PSS impacts on the real section of the critical LFO mode. As a result, if the DTI magnitude is larger, the PSS can contribute more damping torque, resulting in a more significant increase in damping of essential LFO mode. In view of this, this work has proposed the optimal placement of PSS based on the highest DTI magnitude.

The steps for calculating the DTI of each synchronous generator for the power system's dominant oscillation mode of interest are as follows:

1. Identify the Dominant Oscillation Mode:

    - Perform modal analysis of the multi-machine power system to determine the LFO modes and identify the dominant oscillation mode based on its frequency and damping ratio.

2. Calculate the Forward Path:

    - Compute the forward path of each synchronous generator in the power system for the dominant oscillation mode of interest using (2.9).

3. Determine the Damping Torque:

    - Evaluate the damping torque produced by the PSS for the LFO loop of each synchronous generator in the power system using (2.16d).

4. Calculate Total Damping Enhancement:

- Determine the total damping enhancement of the dominant LFO mode of interest provided by the PSS for the power system using (2.17).

5. Compute the Damping Torque Index :

   - Calculate the DTI for each synchronous generator in the power system for the dominant LFO mode of interest using (2.18).

6. Select the Optimal Generator for PSS Installation:

   - Identify the synchronous generator with the highest DTI value. This generator is selected as the most effective location for PSS installation to maximize damping improvement.

2.5 PSS Design Based on the CDTA Method

The design framework of the PSS depends on installation location, the feedback signal, and parameter adjustment. Under normal operating conditions, the PSS parameters were modified using a phase compensation methodology based on the CDTA method [68, 69], ensuring the power systems LFO mode could be suppressed efficiently. According to [65, 68, 69], the PSS parameters can be modified from From (2.19c) - (2.21). The design scheme of the PSS is explained in Fig. 2.4. The PSS alone contributes damping torque to the multi-machine power network to obtain the appropriate design.

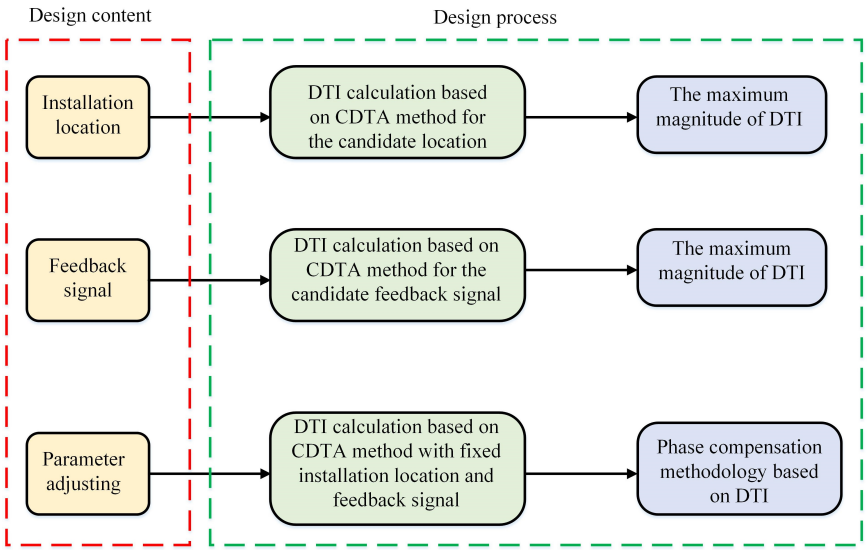

Figure 2.4: PSS design scheme based on DTI.

$$D_{PSSkL} = F_{PSSL}(\lambda_k)\,\gamma_L(\lambda_k)\,T_{PSS}(\lambda_k) \tag{2.19a}$$

$$= T_L\angle\varphi_L T_{PSS}\angle\phi \tag{2.19b}$$

$$= |T_L T_{PSS}|\cos(\varphi_L + \phi) \tag{2.19c}$$

$$\phi = -\varphi_L, |T_{PSSL}| = \frac{D_{PSSkL}}{|F_{PSSL}|} \tag{2.20}$$

From (2.5), the time constant of the lead-lag block can be calculated as

$$\begin{aligned} K_1\frac{j\omega_k T_1 + 1}{j\omega_k T_2 + 1} &= |T_{PSSL}|\angle -\frac{\varphi_L}{2} \\ K_2\frac{j\omega_k T_3 + 1}{j\omega_k T_1 + 1} &= 1\angle -\frac{\varphi_L}{2} \end{aligned} \tag{2.21}$$

where $T_{PSS}\angle\phi = T_{PSS}(\lambda_k)$, PSS gain, $K_{PSS} = K_1 K_2$ and the frequency of critical LFO mode is ω_K.

2.6 WADC Design Framework

Fig. 2.5 depicts the general structure of a WADC designed for a multi-machine power system. The input signals of the WADC are obtained from a PMU. The WADC is designed to dampen a dominant LFO mode by sending an additional damping control signal as feedback to the excitation system of the SG. The time delays in remote signals collected from the wide-area measurement system and other sources, such as control law computation and sample measurements, are simplified into a single delay at the feedback loop, as shown in Fig. 2.5.

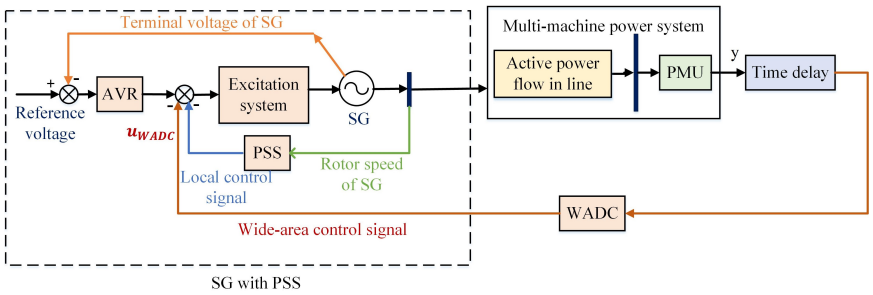

Figure 2.5: Structure of WADC.

2.6.1 Model reduction

Designing a controller based on a full-order model of a multi-machine power system is complicated and computationally inefficient. As a result, a reduced-order model that captures the relevant dynamics of the system and approximates the full-order system is applied to the WADC design. In this analysis, the balanced truncation technique [70] is applied to compute a reduced-order approximation model of a power system by ignoring states with a relatively low impact on the overall system response. The Hankel singular values of $G(j\omega)$ given by [71] are used to calculate state contributions.

$$\sigma_i = \sqrt{\lambda_i(PQ)} \tag{2.22}$$

where $\lambda_i(PQ)$ is the ith largest eigenvalue of (PQ) and P, Q are the results of the following Lyapunov equalities:

$$\begin{cases} PA^T + AP + BB^T = 0 \\ QA + A^TQ + C^TC = 0 \end{cases} \tag{2.23}$$

where, A, B, and C are system state, input, and output matrices.

2.6.2 Feedback signal selection

The Geometric Measure of Observability (GMO) measures the visibility of oscillation mode on a given output [72]. The GMO $gm_{oj}(k)$ associated with mode k is given by

$$gm_{oj}(k) = \frac{|c_j\varphi_k|}{\|\varphi_k\| \, \|c_j\|} \tag{2.24}$$

where φ_k is the right eigenvector of the k^{th} oscillation mode, C_j is the jth row of C, $\|.\|$ and $|.|$ are the euclidean norm and modulus of the matrix, respectively.

The selected output feedback signal should have a high degree of observability of the modes of interest. WADC feedback signal is considered based on the GMO measure of candidate signals to dominant oscillation modes. The signal that has the largest GMO measure and the fewest interactions with other oscillation modes is selected as the feedback signal for WADC.

2.6.3 Design of wide-area damping controller

The commonly used phase compensation Wide-Area Damping Controller (WADC) from [73] is designed in this work to damp dominant oscillation modes by providing a supplementary damping control signal to the excitation system of the SG. The WADC has two lead-lag elements, and its transfer function is as follows

$$G_{WADC}(s) = K_{WADC}\frac{sT_w}{1+sT_w}\left(\frac{1+T_1 s}{1+T_2 s}\right)^2 \tag{2.25}$$

The parameters of the wide-area damping controller are designed using the residue method, and the study test system is linearized under normal operating conditions. T_w is typically set to 3-10s, and K_{WADC} is the gain of the WADC.

2.7 Flowchart of the Proposed Method

Fig. 2.6 shows the proposed method's flowchart.

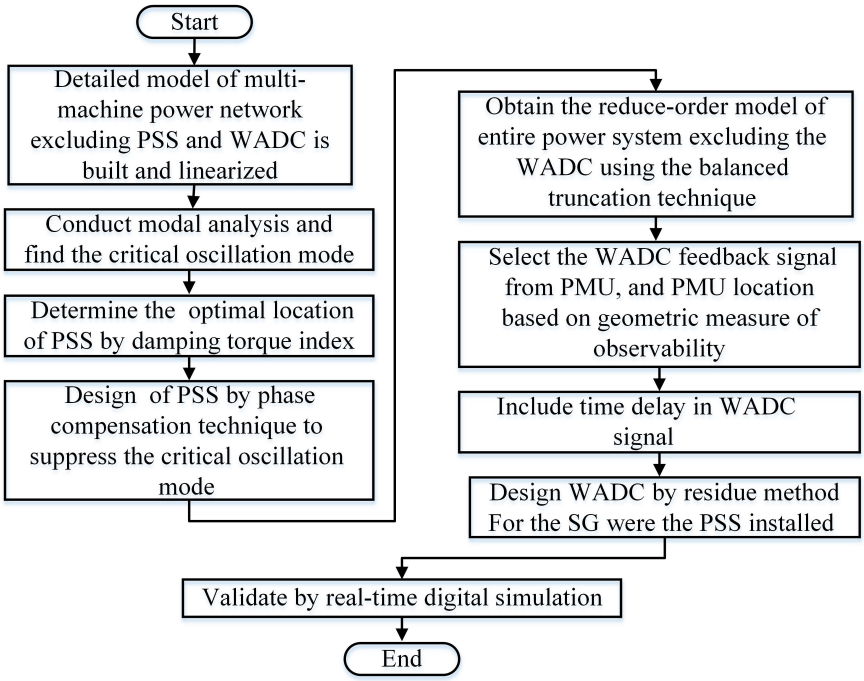

Figure 2.6: Flowchart of the proposed method.

Different steps of the flowchart of the proposed method in Fig. 2.6 is explained as follows:

1. Detailed Model of Multi-Machine Power Network Excluding PSS and WADC

- A detailed dynamic model of the multi-machine power network is developed, excluding the PSS and WADC, to establish a baseline for analyzing system dynamics.
- The system is linearized around its operating point to obtain a state-space representation, which is essential for eigenvalue analysis and control design.

2. Conduct Modal Analysis and Identify the Critical Oscillation Mode

   - Eigenvalue analysis is performed to determine the oscillatory modes of the system.
   - The critical oscillation mode is identified on the basis of its frequency and damping ratio.

3. Determine the Optimal Location of PSS Using DTI

   - The Damping Torque Index is calculated for all synchronous generators in the study system using (2.18).
   - Generators with higher DTI values are identified as having the greatest potential to enhance the damping of the critical mode and are selected for PSS placement.

4. Design PSS Using Phase Compensation Technique

   - The PSS is designed for the selected generators using the phase compensation technique, with its parameters tuned according to (2.21).

5. Obtain a Reduced-Order Model of the Entire System

   - The full system model is reduced using the balanced truncation technique, which preserves the dynamics of the critical modes while simplifying the design process for WADC.
   - This reduced model is used to improve computational efficiency during controller design.

6. Select WADC Feedback Signal and PMU Location

- The appropriate PMU location of the study system is determined based on the geometric measure of observability using (2.24), which ensures the critical mode is effectively monitored.
- The feedback signal with the highest observability of the critical mode is chosen for the WADC design.

7. Include Time Delay in WADC Signal

   - Wide-area control signals inherently involve communication delays due to signal transmission over large distances.
   - The communication time delay is included in the WADC design to ensure robustness under realistic operating conditions.

8. Design WADC Using Residue Method

   - The WADC is designed using the residue approach, with its transfer function provided in (2.25).
   - The WADC is coordinated with the synchronous generator where the PSS is optimally located, as identified by the DTI.

9. Validation by Real-Time Digital Simulation

   - The dynamic simulation response of the study system, incorporating the proposed controller, is validated using a Real-Time Digital Simulator to assess its damping performance.

2.8 Case Study

This study proposed a DTI based on the CDTA method to determine the optimal PSS location to dampen the LFO in the MMPN. The design of the PSS was based on the CDTA method, and its parameters were adjusted by the phase compensation methodology. The proposed approach has been validated on a three-machine IEEE 9-bus system and a five-machine IEEE 14-bus system. Simulations were carried out in MATLAB software. Simulation results were validated on an RTDS RSCAD 5.012. Results obtained on two test systems are presented below.

2.8.1 IEEE 9-bus three machine power systems

The single-line layout of IEEE 9-bus three-machine power systems is illustrated in Fig. 2.7. The test system parameters can be found in [64, 74]. The details of the system are given in Appendix-A. This system is used to analyze electro-mechanical oscillations in power systems. A fourth-order flux decay model expresses each SG, and every SG has a fast static exciter with no PSS.

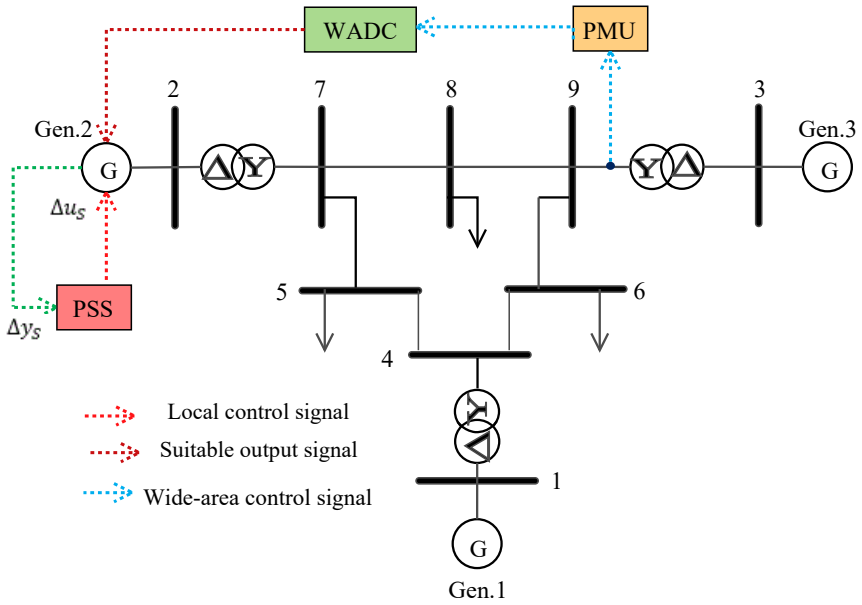

Figure 2.7: Single line layout of IEEE 9-bus power system with optimal location of PSS and WADC.

2.8.1.1 Modal analysis

The eigenvalue analysis (modal analysis) is carried out in a non-linear test system linearized around the normal operating point. The eigenvalues associated with damping ratios, oscillation frequency, and oscillation mode are shown in Table 2.1. This power system test network has two lightly damped LFO modes: M1 (local oscillation) and M2 (inter-area oscillation). The damping ratio of oscillation modes M1 and M2 are less than 5%. Mode M2 is considered critical mode of interest due to low damping ratio.

2.8.1.2 Mode shape and participation factor

The eigenvalue of the critical LFO mode M2 is $-0.19959 \pm j5.9304$. The critical LFO mode M2, i.e., inter-area oscillation mode, is illustrated in Fig. 2.8 with its SG rotor

Table 2.1: Oscillation modes and damping ratios of study case-1

Oscillation mode	**Eigenvalues**	**Damping ratio (%)**	**Frequency (Hz)**
M1	$-0.3054 \pm j8.842$	**3.452%**	1.4073
M2	$\mathbf{-0.1995 \pm j5.9304}$	**3.363%**	**0.9438**

speed-related mode shapes and Participation Factor (PF) plot. The critical LFO mode M2 depicts the potential oscillation of SG G2-G3 swinging against G1, as seen in Fig. 2.8(a). In critical LFO mode, the PF plot likewise shows that SG1 is the most consistent SG.

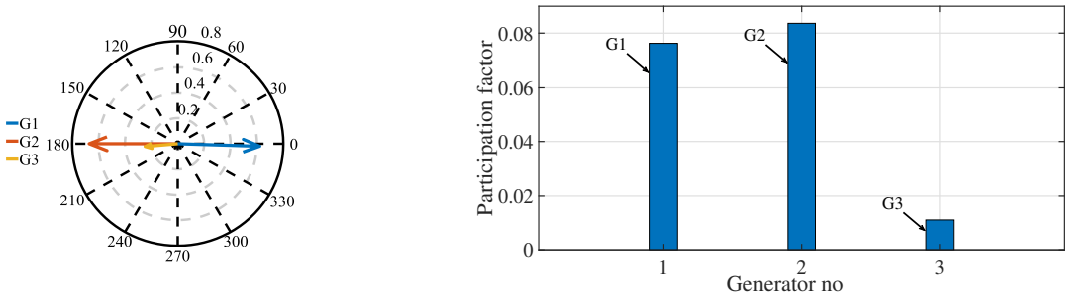

(a) (b)

Figure 2.8: Critical LFO mode M2. (a) SG rotor speed-related mode shapes and (b) Participation factor plot

2.8.1.3 Selection of the PSS installing locations

2.8.1.3.1 Sensitivity index

Calculating the sensitivity of eigenvalues of critical oscillation modes with respect to the addition of extra damping torque in LFO mode can be used to determine the PSS installation position in MMPN LFO analysis.

The Sensitivity Index (SI) of λ_k to the addition of damping torque with the L^{th} SG can be defined as

$$S_{kL} = \frac{\partial \lambda_k}{\partial D_{PSSkL}} \tag{2.26}$$

The steps for calculating the sensitivity index of each synchronous generator for the power system's dominant oscillation mode of interest are as follows:

1. Determine the Dominant Oscillation Mode of the Power System:

- Conduct modal analysis of the multi-machine power system to identify the dominant LFO modes.

2. Addition of Artificial Damping:

   - Introduce an artificial damping term to the electromechanical oscillation loop of each synchronous generator of the power system to simulate the effect of PSS installation.

3. Sensitivity Index Calculation:

   - The sensitivity index of each synchronous generator of the power system for the dominant oscillation mode of interest is calculated using (2.26).

4. Select the optimal synchronous generator for PSS Installation:

   - Synchronous generators with the highest sensitivity index of the power system are identified as the optimal location for PSS installation.

The SI of the generators G1,G2, G3 corresponding to the critical oscillation mode $\lambda_k = -0.1995 \pm j5.9304$ are listed in Table 2.2. It is obtained from Table 2.2 that the SI of G1 is 0.0391, which is higher than the SI of other SGs and therefore, SG-1 represents the most active synchronous generator to LFO mode of interest. Therefore, G1 is chosen as the optimal PSS location in the MMPN to damp out the critical LFO mode M2.

Table 2.2: Sensitivity and damping torque index of study case-1

PSS location	**G1**	**G2**	**G3**
SI	**0.0391**	0.0378	0.0016
DTI	0.0451	**0.1950**	0.0257

2.8.1.3.2 Damping Torque Index

The PSS is placed where appropriate SG can stabilize the critical LFO mode ($-0.1995 \pm j5.9304$) and assess the DTI related to critical LFO mode M2 for generators G1 to G3. The DTI evaluated results are listed in Table 2.2. It is observed from Table 2.2 that the DTI magnitude of G2 is 0.1950, which is much higher than DTI for other SGs, and the PSS can contribute more damping torque, resulting in a considerable damping rise of

the essential LFO mode M2. Therefore, G2 is chosen as the optimum PSS installation position in the MMPN to damp out the critical LFO mode M2. As shown in Fig. 2.9, the PSS installed on G2 will impact the critical LFO mode of interest in M2.

From Table 2.2, the optimum location of PSS to suppress LFO mode of interest M2 in the IEEE 9-bus power network based on SI is SG-1, while SG-2 is considered best location based on DTI. SI indicates how closely a generator is related to the LFO mode of interest and can be used to determine where the PSS should be installed. However, SI is ineffective for estimating the contribution of damping torque from the power system damping controller to each SG in the LFO mode of interest. So, proposed DTI based PSS installation is better compared to SI based installation. Therefore, the PSS optimum installation position in the MMPN to damp out the critical LFO mode of interest M2 is selected as SG-2.

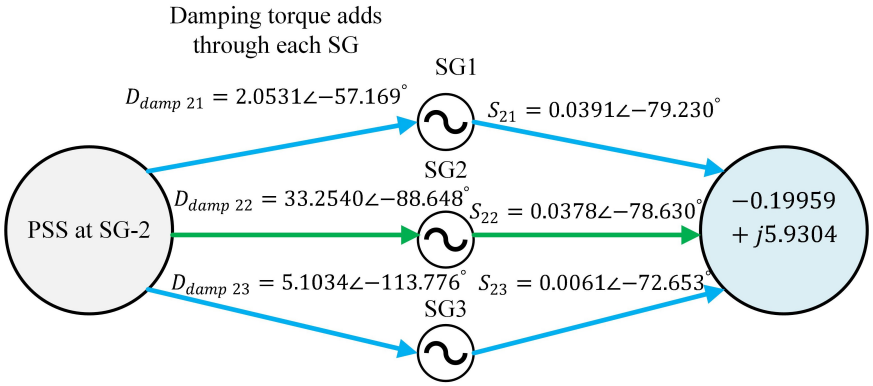

Figure 2.9: The PSS is to be inaugurated on G2 to affect the critical LFO mode M2.

2.8.1.3.4 Design of the PSS

On behalf of DTI, the PSS is installed on SG-2 to reduce LFO in the MMPN using the CDTA approach. In nominal operating conditions, the forward path after the PSS stabilizing signal to the SG critical LFO loop can be obtained at the critical mode of angular frequency.

$F_{PSSkL(\lambda_k)} = 0.7843 - j33.2448 = 33.254\angle -88.648°$ where $\lambda_k = -0.19959 + j5.9304$. The PSS parameters are adjusted from (2.19c) to (2.21) by phase compensation methodology to compensate for the phase lag angle $\phi_L = -88.648°$ after the PSS controlling signal is introduced to the SG critical LFO loop. Adjusted PSS parameters are: lead-lag block time constant is $T_2 = T_4$ are 0.02 s, and reset filter time constant T_w is 10 s at that

time, parameters of PSS adjusted as $K_{PSS} = 1.2152, T_1 = T_3 = 0.2088$ s through the phase compensation technique [65, 68, 69].

To justify the efficacy of the PSS, Table 2.3 provides the numerical results of eigenvalues of multi-machine power systems at critical oscillation mode (other LFO modes are not cataloged) without and with the PSS.

Table 2.3: Eigenvalues of study case-1

	Mode	**Damping ratio** (%)	**Eigenvalues**
Without the PSS	M2	3.363	$-0.1995 \pm j5.9304$
With the PSS	M2	**7.663**	$\mathbf{-0.4220 \pm j5.4903}$
With the WADC	M2	**14.024**	$\mathbf{-0.805 \pm j5.74}$

.

From Table 2.3, suppression of critical LFO mode of interest M2 in the IEEE 9-bus power network by incorporating PSS in SG-2 is observed.

2.8.1.4 WADC framework for study case-1

The modal analysis results for the IEEE 9-bus test system are shown in Table 2.1. Mode M2 is a critical oscillation mode, as can be seen. Because it has a comparatively small damping ratio of 0.03363 and an oscillation frequency of 0.9438 Hz, it is thought to be the crucial mode whose damping is intended to be improved by the WADC.

2.8.1.4.1 Model-order reduction for study case-1

Fig. 2.10 depicts the Hankel singular value of the IEEE 9-bus study test system 12^{th} order linearized model that reveals that the contribution up to state-4 in the output/input behaviour is significantly higher than the contribution of the other remaining states, indicating that the system's order can be lowered during the controller design phase. Except for the WADC, the open-loop system is a 12^{th}-order system. The Balanced Truncation (BT) technique is used to construct a reduced-order model using P_{3-9} as output and u_{WADC} as the input signal.

The frequency responses of the full-order system and reduced-order systems of various orders are depicted in Fig. 2.11. Over the low-frequency oscillation range of 0.2 to 2.5 Hz, the frequency response of the reduced-order system is shown to be highly close

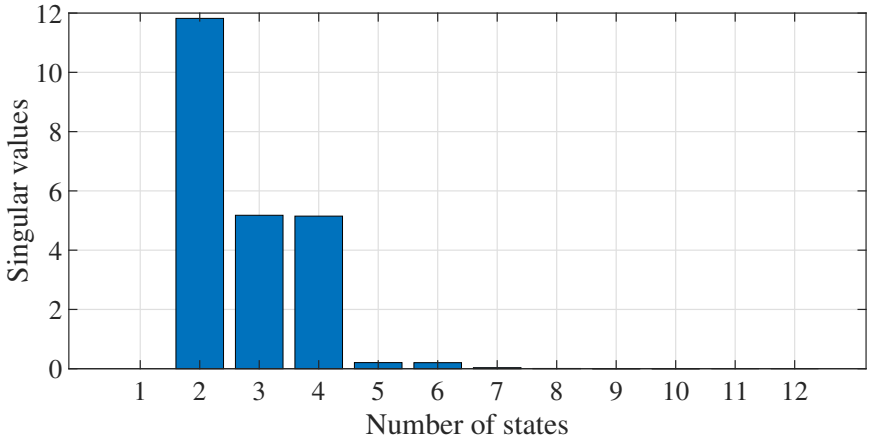

Figure 2.10: Hankel singular values corresponding to state linearized model of the IEEE 9-bus system.

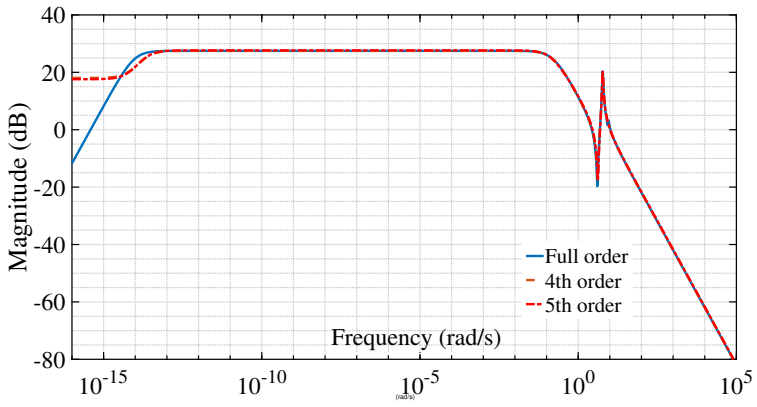

Figure 2.11: Frequency response of reduced-order and full-order models of the IEEE 9-bus system.

to that of the full-order system when the system order is 4 and more. As a result, the IEEE 9-bus test system can be reduced to a 4^{th}-order system for the study of dominant oscillation mode. The 4^{th}-order open-loop transfer function of the IEEE 9-bus test system is as follows:

$$H_{9bus}(s) = \frac{N_{9bus}(s)}{D_{9bus}(s)} \tag{2.27}$$

where, $N_{9bus}(s) = 8s^3 + 2.363s^2 + 136.5s + 9.639 \times 10^{-13}$

$D_{9bus}(s) = s^4 + 0.5617s^3 + 35.21s^2 + 5.78s - 1.204 \times 10^{-13}$

2.8.1.4.2 Feedback signal selection for study case-1

Fig. 2.12 shows the $gm_{oj}(k)$ calculation results for all active powers in transmission lines for critical oscillation mode M2. It can be observed that line 7-8 have high observability of mode M1, but line 3-9 have high observability of dominant oscillation mode M2. The WADC's remote feedback signal is chosen from the active power flows in line 3-9. As a result, PMUs are installed at bus 9 to monitor the active power flow in those lines.

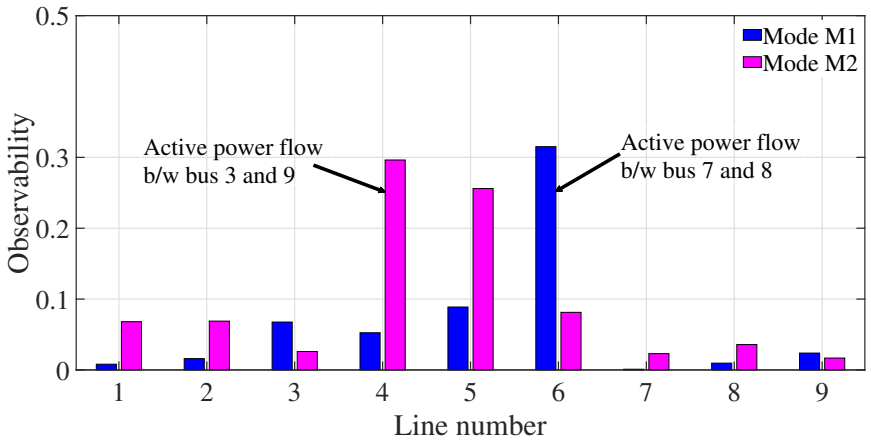

Figure 2.12: Geometric measurement of observability of IEEE 9-bus system.

2.8.1.4.3 Design of the WADC for study case-1

The design of WADC by residue method to compensate for the phase lag angle $\phi_L = 89.0598°$ in dominating oscillation mode M2 is considered with 100 ms time delay in the wide-area signal. The parameter of WADC is depicted in Fig. 2.13. The lead-lag compensation part of the WADC is given as follows: $T_1 = 0.4028s, T_2 = 0.07073, T_w = 10s$ and gain of WADC is $K_{PCWADC} = 0.309$. The output of the WADC is limited by ± 0.1pu to avoid influence from the excitation system of SG. To justify the efficacy of the WADC, Table 2.3 provides the numerical outcomes of eigenvalues for the critical oscillation mode (other LFO modes are not cataloged).

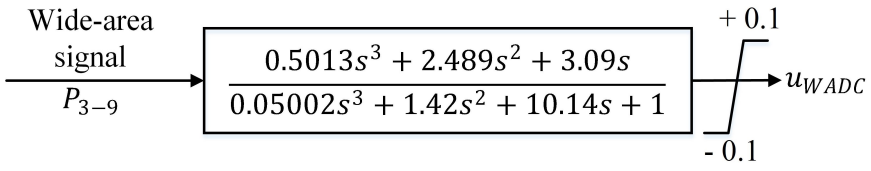

Figure 2.13: Parameter of WADC in IEEE 9-bus system.

2.8.1.5 Real-time simulation results

The modal analysis results of study test systems are verified by non-linear time-domain simulation using the RTDS with the graphical user interface of RSCAD 5.012. The GTSYNC card on the RTDS allows it to receive a one-pulse-per-second signal from the satellite via a GPS clock. This signal is used to synchronize the GPS clock with the software PMUs, which are referred to as GTNET PMUs in the RTDS. The simulation's data is delivered to GTNET PMUs. The data from the PMU is sent to the WADC in the RSCAD draft file, and the controller's output is fedback into the simulation. The framework of the real-time simulation platform has been illustrated in Fig. 2.14. The non-linear time-domain simulation has been carried out in transmission mode with the main time step (dt) of 50μs.

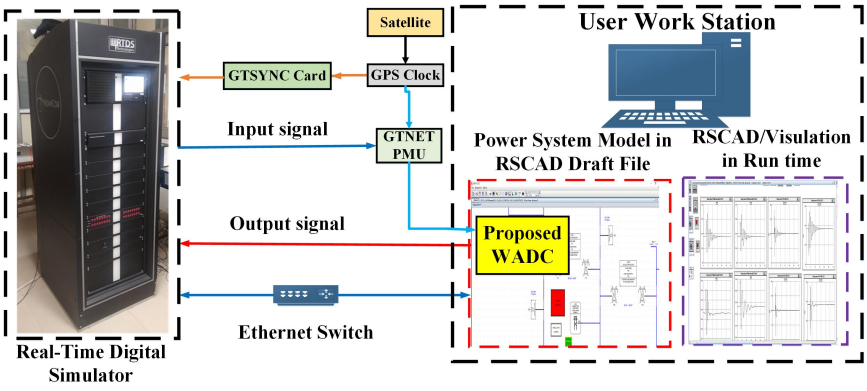

Figure 2.14: Real-time simulation framework.

The results of a non-linear time-domain simulation of the IEEE 9-bus power network when a three-phase short circuit happened at bus five at 0.1 s are shown in Fig. 2.15. It is observed from Fig. 2.15(a) and Fig. 2.15(c) that PSS installation at G2 results in better damping of rotor speed and line flow oscillations compared to PSS placement at G1 or G3. It is observed further from Fig. 2.15(b), Fig. 2.15(d), and Fig. 2.15(e) that PSS in combination with WADC is very effective in damping critical mode of oscillations.

Table 2.3 shows the eigenvalue analysis outcomes for study test case-1, which is a reduced-order model-based WADC for the synchronous generator with the optimal location of PSS, including time delay. As a result of the foregoing, WADC provides higher damping performance than the optimal location of the PSS on the synchronous generator. When WADC is installed on the SG-2, the rotor speed and active power flow in line P_{3-9} are shown in Fig. 2.15(b) and Fig. 2.15(e), respectively.

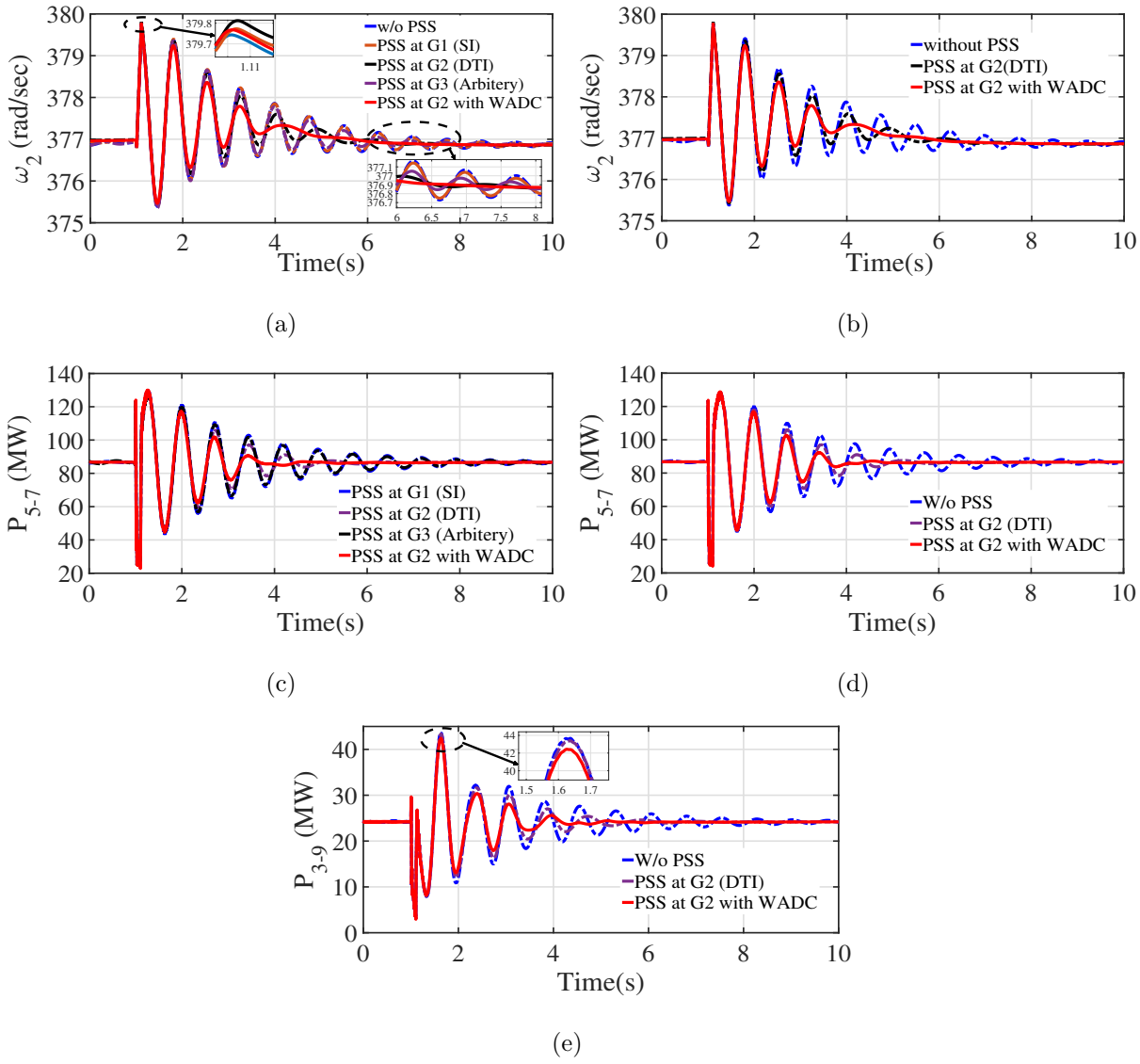

Figure 2.15: Real-time digital simulation results of IEEE 9-bus system; (a) comparative rotor speed of G2 with different location of PSS, (b) rotor speed of G2, (c) comparison of line active power of line (5-7), (d) active power of line (5-7), and (e) active power of line (3-9).

Table 2.3 and Fig. 2.15 show that the WADC with the optimal location of PSS provides better damping performance to in critical oscillation mode than the optimal location of the PSS inaugurated on SG-2 without WADC.

2.8.2 IEEE 14-bus five machine power systems

To further determine the achievement of the proposed approach when realizing a larger sample of the multi-machine power networks, we studied IEEE 14-bus five machines power

systems, as shown in Fig. 2.16. Parameters of the test system are given in [75]. The details of the system are given in Appendix-B. A fourth-order flux decay model is considered for each SG, and every SG has a fast static exciter with no PSS. We proposed a DTI index based on the CDTA approach to finding the optimal positions of the PSS to damp out power system LFO in a multi-machine system. The design of the PSS is based on the CDTA method and parameters adjusted by phase compensation methodology [65, 68, 69].

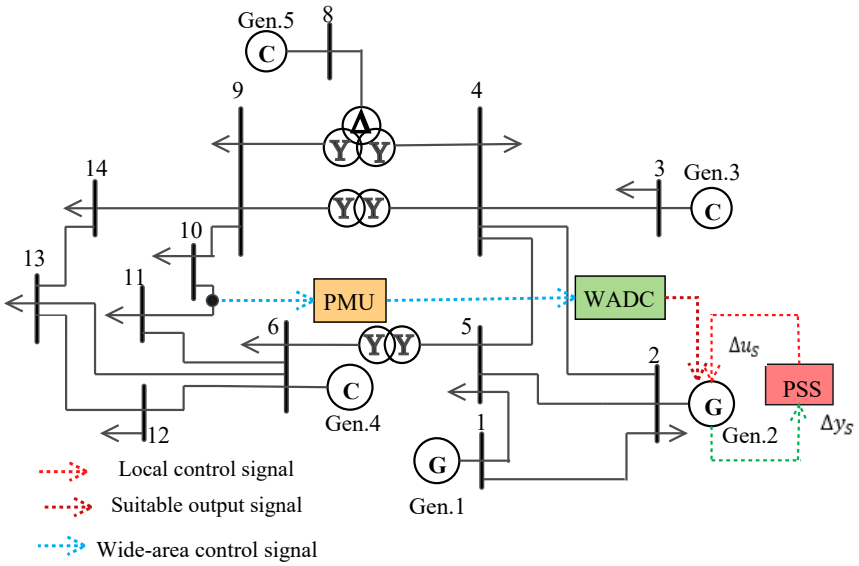

Figure 2.16: Single line layout of IEEE 14-bus power system with optimal location of PSS and WADC.

2.8.2.1 Modal analysis

Table 2.4 illustrates the eigenvalues corresponding to oscillation frequency, damping ratios, and oscillation modes in the IEEE 14-bus five machine test system, linearized around the nominal operating point. This multi-machine power system has four lightly damped oscillation modes: M1, M2, M3, and M4. The damping ratio of all oscillation modes are less than 5% except oscillation mode M4. Mode M1 is considered critical mode of interest due to lowest damping ratio.

.

2.8.2.2 Mode shape and participation factor

The eigenvalues of the critically damped LFO modes M1 are $-0.1756 \pm j11.58$. The critical LFO mode M1, i.e., local-area oscillation mode, is illustrated in Fig. 2.17 with its SG rotor speed-related mode shapes and PF plot. The critical LFO mode M1 depicts

Table 2.4: Oscillation modes and damping ratios of study case-2

Oscillation Mode	**Eigenvalues**	**Damping ratio (%)**	Frequency (Hz)
M1	**$-0.11756 \pm j11.58$**	**1.5162**	**1.843**
M2	$-0.2169 \pm j11.389$	1.9043	1.8127
M3	$-0.1773 \pm j10.799$	1.6141	1.7187
M4	$-0.8634 \pm j6.5047$	13.159	1.0353

the potential oscillation of all SG swinging against G2, as seen in Fig. 2.17(a). In critical LFO mode, the PF plot demonstrates that G2 is the most consistent SG.

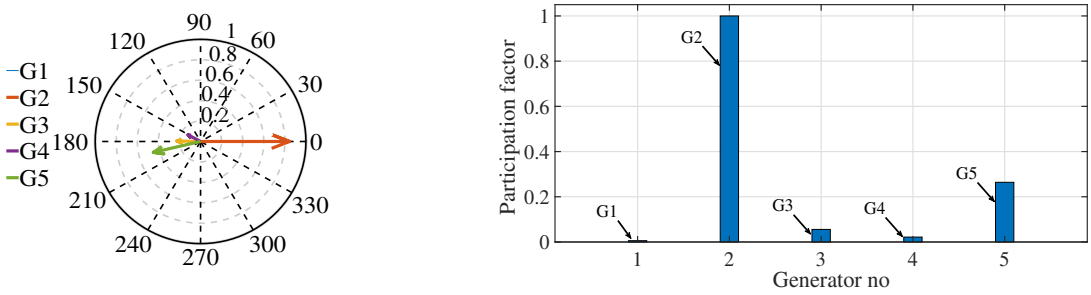

(a) (b)

Figure 2.17: Critical LFO mode M1; (a) SG rotor speed-related mode shapes and (b) participation factor plot.

2.8.2.3 Selection of the PSS installing locations

2.8.2.3.1 Sensitivity index

The SI evaluated results of the critical oscillation mode $\lambda_k = -0.1756 \pm j11.58$ are listed in Table 2.5. It is observed that the SI of G2 is 0.0610, which is higher than SI for any other SG. As a result, G2 is chosen as the optimal PSS location in the IEEE 14-bus power network to dampen out the critical LFO mode M1.

Table 2.5: Sensitivity and damping torque index of study case-2

PSS location	**G1**	**G2**	**G3**	**G4**	**G5**
SI	0.0003	**0.0610**	0.0034	0.0013	0.0161
DTI	0.0050	**0.4334**	0.0043	0.000592	0.0153

.

2.8.2.3.2 Damping torque index

The DTI related to critical oscillation mode M1 for each SG is carried out to find the appropriate installation location of the PSS for relevant SG for stabilizing the critical LFO mode M1 ($-0.1756 \pm$ j11.58). The DTI numerical results are listed in Table 2.5. The DTI magnitude of G2 is 0.4334, which is larger than that of other SG, and the PSS can provide additional damping torque, resulting in a more damping increase of the critical LFO mode M1. Therefore, G2 is selected for the optimal installation location of PSS in the IEEE 14-bus power network to dampen out the associated critical oscillation mode M1.

From Table 2.5, SG-2 is the optimum location of PSS to suppress the LFO mode of interest M1 in the IEEE 14-bus power network based on SI as well as based on DTI.

2.8.2.3.3 Design of the PSS

The PSS is installed on SG-2 in the IEEE 14-bus power network to suppress the LFO. Under nominal operating conditions, the forward path after the PSS stabilizing signal to the SG critical LFO loop can be estimated in the frequency of critical oscillation mode.

$F_{PSSkL(\lambda_k)} = -0.5975 - j6.5312 = 6.5585\angle - 95.226^\circ$

where $\lambda_k = -0.1756 + j11.58$.The PSS parameters are adjusted using a phase compensation technique [65, 68, 69] to compensate for the phase angle lag $\phi_L = -95.226^\circ$. PSS parameters after adjustment are: lead-lag block time constant is $T_2 = T_4$ are 0.02 s, and reset filter time constant T_w is 10 s at this instant of time, parameters of PSS are adjusted through phase compensation technique as $K_{PSS} = 2.8179, T_1 = T_3 = 0.1535$ s.

Table 2.6 shows the computational results of eigenvalues for the critical LFO mode (other LFO modes are not cataloged) without and with the PSS to justify the PSS effectiveness.

. From Table 2.6, suppression of critical LFO mode of interest M1 in the IEEE 14-bus power network by incorporating PSS in SG-2 is observed.

Table 2.6: Eigenvalues of study case-2

	Mode	**Damping ratio** (%)	**Eigenvalues**
Without the PSS	M1	1.5162	$-0.11756 \pm j11.58$
With the PSS	M1	**5.5832**	$\mathbf{-0.6079 \pm j10.871}$
With the WADC	M1	**10.4**	$\mathbf{-1.19 \pm j11.3}$

2.8.2.4 WADC framework for study case-2

Table 2.4 shows the modal analysis outcomes for the IEEE 14-bus test system. As can be observed, mode M1 is a critical oscillation mode. It is a low-frequency oscillation mode whose damping is intended to be increased by the WADC since it has a comparatively small damping ratio of 1.5162 and an oscillation frequency of 1.843 Hz.

2.8.2.4.1 Model-order reduction for study case-2

The Hankel singular value of the IEEE 14-bus study test system is shown in Fig. 2.18. The contribution up to state-10 in the output/input behaviour is much higher than that of the remaining states in the 20^{th}-order linearized model, showing that the system's order can be reduced during the controller design phase. The open-loop system, with the exception of the WADC, is a 20^{th}-order system. With P_{10-11} as the output signal and u_{WADC} as the input signal, the BT approach is utilized to build a reduced-order model.

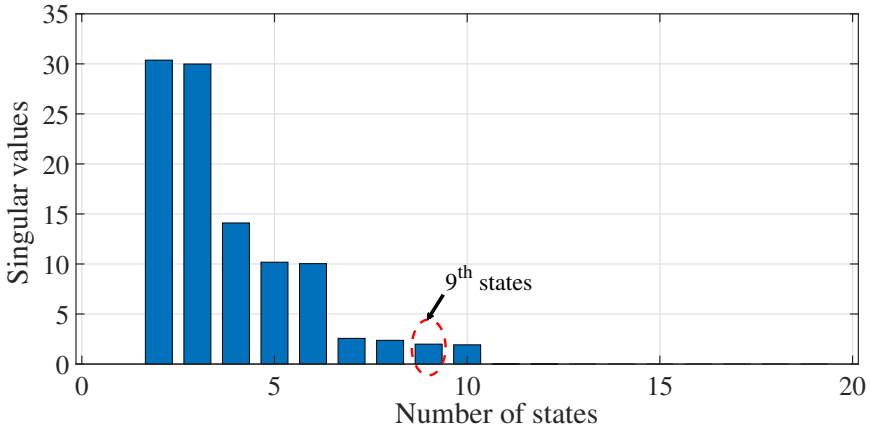

Figure 2.18: Hankel singular values corresponding to IEEE 14-bus system state linearized model.

Fig. 2.19 depicts the frequency responses of full-order and reduced-order systems of various orders. When the system order is more than 6, the frequency response of the

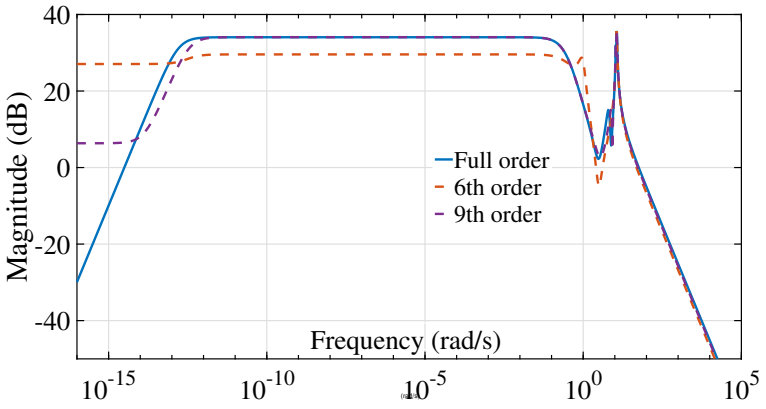

Figure 2.19: Frequency response of reduced-order and full-order models of the IEEE 14-bus system.

reduced order system is demonstrated to be very close to that of the full order system over the low-frequency oscillation band of 0.2 to 2.5 Hz. As a result, the IEEE 14-bus test system can be reduced to a 9^{th}-order system for the analysis of the dominant oscillation mode. The 9^{th}-order open-loop transfer function of the IEEE 14-bus test is as follows:

$$H_{14bus}(s) = \frac{N_{14bus}(s)}{D_{14bus}(s)} \tag{2.28}$$

$$\begin{aligned} N_{14bus}(s) = {} & 51.58s^8 + 122.2s^7 + 1.034 \times 10^4 s^6 + 1.965 \\ & \times 10^5 s^5 + 5.32 \times 10^5 s^4 + 6.941 \times 10 s^3 \\ & + 4.27 \times 10^6 s^2 - 5.47 \times 10^6 s + 7.934 \\ & \times 10^{-8} \\ D_{14bus}(s) = {} & s^9 + 1.94s^8 + 313.8s^7 + 432.4s^6 + 3.147 \times 10^4 s^5 \\ & + 2.449 \times 10^4 s^4 + 9.876s^3 + 8.181 \\ & \times 10^4 s^2 - 1.082 \times 10^5 s - 3.724 \times 10^{-8} \end{aligned}$$

2.8.2.4.2 Feedback signal selection for study case-2

For critical oscillation mode M1, the $gm_{oj}(k)$ calculation outcomes for all active powers in transmission lines are shown in Fig. 2.20. Line 10-11 have maximum observability for critical oscillation mode M1. The remote feedback signal for the WADC is selected from the active power flows in line 10-11. PMUs have been installed at bus 11 to monitor the active power flow in lines as a result.

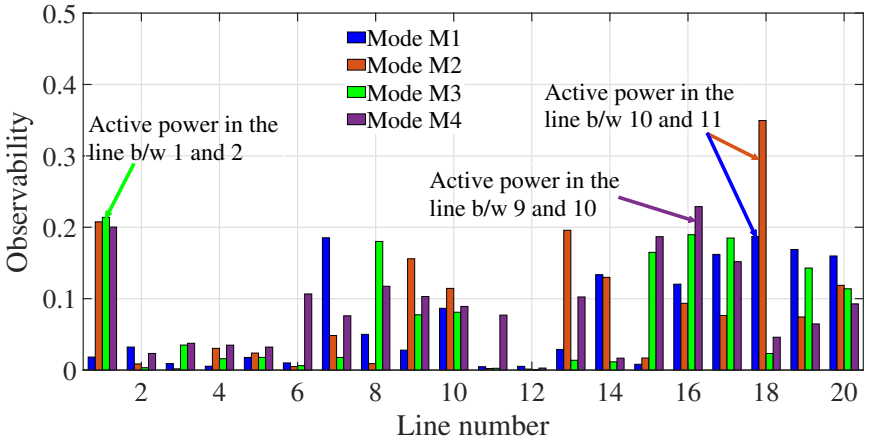

Figure 2.20: Geometric measurement of observability of IEEE 14-bus system.

2.8.2.4.3 Design of the WADC for study case-2

The WADC provides a supplementary damping control signal to the SG's excitation system; it is designed using the residue method to adjust for the phase lag angle $\phi_L = -21.4934°$ in dominating oscillation mode M1 with considering 100 ms time delay in the wide-area signal. The lead-lag compensation part of the WADC has the following parameters: $T_1 = 0.06816s, T_2 = 0.1258, T_w = 10s$, and the gain of the WADC is $K_{PCWADC} = 0.0431$. The parameter of WADC is depicted in Fig. 2.21. To avoid the effect from the SG's excitation system, the WADC's output is limited to ±0.1pu.

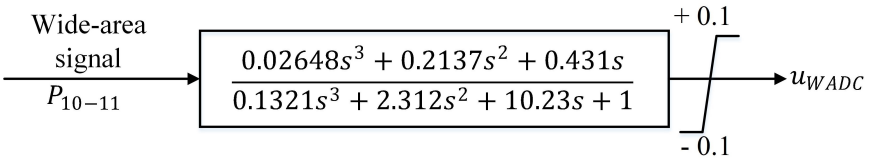

Figure 2.21: Parameter of WADC in IEEE 14-bus system.

Table 2.6 shows the numerical results of eigenvalues in a critical oscillation mode to demonstrate the usefulness of the WADC (other LFO modes are not cataloged).

The results of a non-linear time-domain simulation of the IEEE 14-bus power network when a three-phase short circuit happened at bus four at 0.1 s are shown in Fig. 2.22.

Fig. 2.22(a) shows the PSS at G2 contributes more damping to suppress the critical oscillation mode (viz. rotor speed of G2) compared to PSS installation at other generators. Fig. 2.22(c and d) show that the low-frequency power oscillation is effectively suppressed by incorporating PSS at G2.

As indicated in Table 2.6 and Fig. 2.22, it is observed that the PSS incorporation

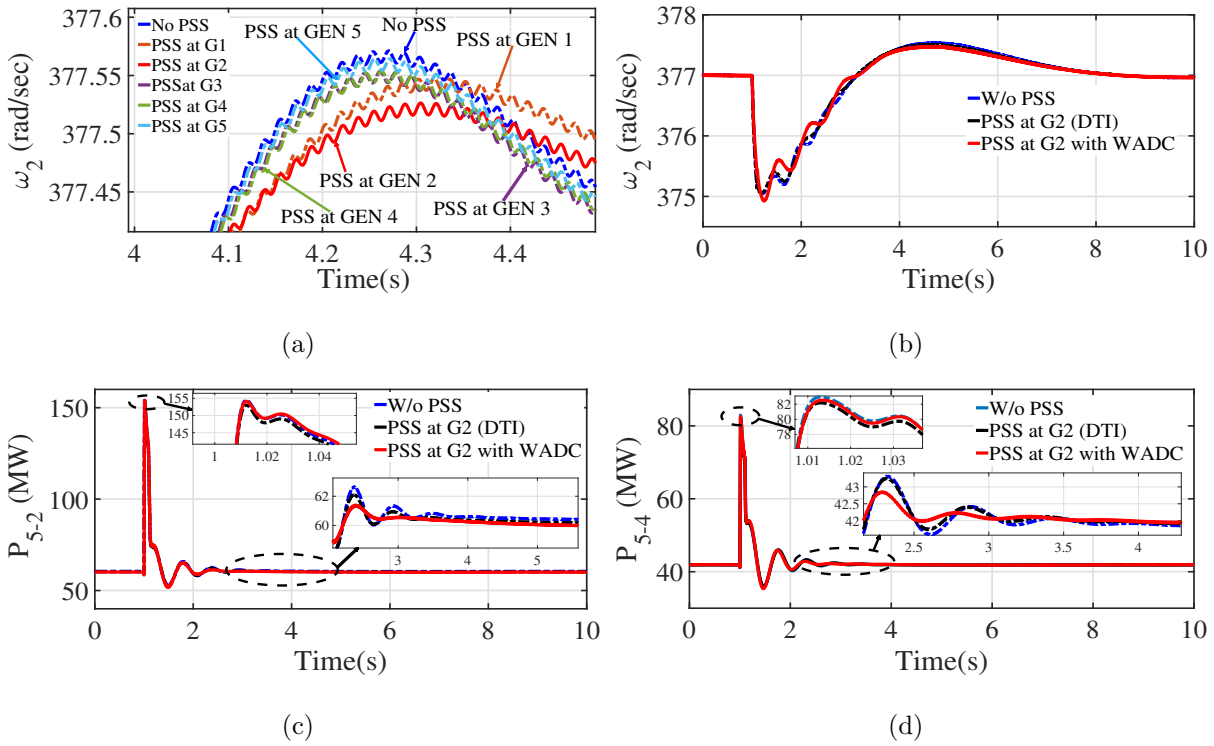

Figure 2.22: Real-time digital simulation results of IEEE 14-bus system; (a) comparative rotor speed of G2 with different locations of PSS, (b) rotor speed of G2, (c) active power of line (5-2), and (d) active power of line (5-4).

effectively suppresses the critical LFO mode in the IEEE 14-bus power network.

The eigenvalue analysis results for study test case-2 for a reduced-order model-based WADC for the synchronous generator with the optimal location of the PSS in the exciter system are shown in Table 2.6. It is observed that WADC with the optimal location of PSS provides higher damping performance than the optimal location of the PSS without WADC, as illustrated in Fig. 2.22 (b, c, and d), and Table 2.6.

2.9 Summary

The proposed DTI based on the CDTA method is presented in this study as part of the selection criteria for the optimal PSS installation location in multi-machine power systems for critical LFO mode damping. The larger magnitude of the DTI under nominal operating conditions is the selection criteria for the PSS location. The design of PSS is based on the CDTA method, and the phase compensation technique adjusts its parameters. Furthermore, the balanced truncation technique is utilized to design a reduced-order

model-based WADC that incorporates a time-varying delay in the wide-area signal for the synchronous generator exciter system with the optimal location of the PSS to analyze the dominant oscillation mode in a multimachine power system. The WADC's input signals from the PMU and the location of the PMU were selected using geometric measures of observability and WADC design parameters based on the residue method. The proposed approach is validated in two-test systems. Simulation results show that WADC with the optimal location of PSS provides better damping performance to critical oscillation mode than the optimal location of the PSS without WADC.